FOS ENTRANCE APERTURE OFFSETS
(Laboratory Calibration Plan 13G)

M. SIRK and R. BOHLIN
SPACE TELESCOPE SCIENCE INSTITUTE

Instrument Science Report CAL/FOS—029
May 1986

Abstract

Offsets between the FOS entrance apertures are determined from spectra obtained with the internal wavelength lamps for both Digicons. The displacement of the spectral lines among the lower, middle and upper aperture locations, respectively, are constant along the diode array and range from 0.0 to 0.17 diode. Non-constant offsets that vary from 0 to 0.1 diode along the diode array are observed when the lower and upper apertures of a pair are compared. The internal accuracy in the determinations of these offsets is typically 0.003 diode.

The application of the methods and results developed here to the overall wavelength calibration strategy is outlined. The aperture offsets are small enough so that other uncertainties dominate with an expected error of ±0.5 diode in the case where no wavelength calibration is obtained with the science data. In the case where a wavelength calibration is obtained, the reduction technique is independent of any aperture offset; and a precision that approaches the accuracy of about 0.02 diode or 5 km s^{-1} for the high dispersion wavelength calibrations may be possible.

I. Introduction

Precise wavelength scales are needed to obtain accurate velocities of lines in astrophysical objects. For this purpose, the FOS has a wavelength calibration lamp, which can illuminate the entrance apertures, whenever the entrance port door is closed. The accuracy of the wavelength scales that can be assigned to a target spectrum is limited by the accuracy to which the wavelength scale of the calibration lamp can be determined, by the accuracy to which a point source can be centered in an aperture, and by any offset that might exist between the calibration lamp spectrum and the spectrum of a perfectly centered external object. This study along with the previous paper by Sirk and Bohlin (1986) addresses the

first question of the accuracy of the wavelength calibration spectra, which is as good as 5 km s^{-1} for the high dispersion (R=1300) gratings. The second question of pointing accuracies will be answered by studies in the HST Science Verification period that are designed to confirm a model of the FOS target acquisition accuracy as a function of stellar brightness, integration time, and slope of sky background. The third question of internal to external spectrograph offsets can be addressed for diffuse external sources in the lab but must await Science Verification data on point sources for final resolution.

Light from the Hubble Space Telescope is focused onto the FOS entrance aperture mechanism which consists of a blank aperture position plus 11 sets of single or paired apertures for each Digicon ranging from 0.1 to 4.3 arcsec projected onto the sky. Figure 1 shows the relative sizes and locations of the apertures. The positions of the apertures when they are rotated into the optical path of the FOS are known to repeat to an accuracy of 0.002 arcsec or $\pm$ 0.6 microns in the focal plane, which results in an error of $\pm$ 0.004 diode on the diode array (Wheatley, Bohlin, and Ford 1983). Although the most accurate wavelength scales for the FOS are determined from the internal Pt-Cr-Ne calibration lamp spectra through the smallest of the lower, upper, and centered apertures (*i.e.* 0.1-PairL, 0.1-PairU, and 0.3 arcsec), offsets between these smallest apertures and the larger ones will cause shifts in the positions of spectral features. For some medium sized apertures (0.25-Pair, 0.25 x 2.0), a direct determination of the wavelength scale can be made from line identification. However, line blending precludes the identifications of enough single lines for the larger apertures ($\geq$ 0.5 arcsec). The general technique of cross–correlation of large aperture spectra with template spectra from the small apertures for determining aperture offsets is discussed in sections II and IV.

The original calibration strategy assumed that there are constant offsets between all apertures and that wavelength scales could be determined by knowing the offsets between the 0.1-PairL aperture and all the other apertures. However, this study shows *differential* offsets in the X direction of a spectrum depending on the aperture location in the Y direction, which is perpendicular to the dispersion. Figures 2 and 3 show offsets *vs.* diode number for two cases. The offsets were found between spectra obtained simultaneously in the lower and upper apertures of a pair. The significant non–zero slopes found from a linear least squares fit indicate differential offsets that are probably caused by a slight change in the magnetic

field. Therefore, three sets of offsets are required for the large apertures: each set is with respect to the smallest lower, middle, and upper aperture.

II. Data and Analysis

Five sets of calibration data are available for determining aperture offsets, as summarized in Table 1.

Table 1

Aperture Offset Calibration Data

Tube	Disperser	Condition	Temperature	Lamp	Date
Blue	G130H	vacuum	-30 C	internal	14–Jul–84
Blue	G130H	vacuum	-10 C	internal	19–Jul–84
Blue	Prism	ambient	20–30 C	external	28–Aug–84
Red	G570H	ambient	20–30 C	external	25–Aug–84
Red	Prism	ambient	20–30 C	external	25–Aug–84

For both tubes, spectra were obtained through all apertures (except the 4.3 arcsec target acquisition aperture) without moving the Filter Grating Wheel. The spectra obtained with the above dispersers were intended to explore the extreme cases but are not optimally suited for determining aperture offsets. The blue tube G130H spectra show virtually no flux from diodes 0 to 100, and the red tube G570H spectra show just a few faint lines between diodes 250 and 512. Should more precise aperture offsets be required in the future, spectra from gratings G270H for the red tube, and G190H or G270H for the blue tube would be ideal as they provide the most uniform distribution of spectral lines across the entire diode array.

The prism spectra cover only 140 of the 512 diodes of the FOS. The region from 3300 to 8000Å has line blending and high countrates (and, thus, uncertainties in the pulse coincidence corrections). The prism data define the worst case line blending problem at the longer wavelengths. If a method for determining aperture offsets works for prism spectra, then the method is likely to work for all other dispersers.

Aperture offsets are determined using a cross–correlation between spectra from the larger apertures and a template spectrum from the smallest apertures. In order to investigate differential effects, the spectra are divided into 20 bins, each of which is 25 diodes wide. Before performing the cross–correlation the spectrum taken through the smaller aperture is smoothed to the resolution of the larger aperture spectrum. For example, if the offset between the 1.0-PairL and 0.1-PairL apertures is to be determined, the 0.1-PairL spectrum is first boxcar smoothed over 11 data points (quarter steps) since the FWHM of the 1.0-PairL aperture is 1 arcsec or 11.4 quarter steps. This smoothing is done to reduce apparent shifts that might be caused by cross–correlating blended spectral lines with unblended lines. Offsets are determined by computing the difference between spectra from the small template aperture in each aperture location (*i.e.* lower, upper, and centered) with spectra from the larger apertures of the same location. Bins containing less than 1800 total counts in the 25 diode bin width are rejected since their cross–correlation curves typically show many maxima. A linear least squares fit is performed on all offset data to check for significant differential offsets. Points that show a 2.5σ residual or larger are also rejected. Figures 4 and 5 show two typical cases of aperture offsets, one for each tube. The dashed lines are the least squares fits and show no significant slopes, indicating that aperture offsets between like aperture locations are constant. The red tube spectra have several bins that repeatably show a large residual. An examination of a spectrum shows that these bins have either no lines or just one bright line on the border of the bin. The mean offset is defined as the average of the remaining bins, and the error in the mean is computed by dividing the RMS scatter by the square root of the number of bins.

III. Results

The mean offsets and their errors for the red tube for both G570 and the prism are listed in Table 2. Offsets for the cold and hot G130H vacuum data sets from the blue tube are presented as Table 3. Table 4 shows the offsets for the blue side prism data. A positive offset indicates that the spectrum as viewed by the indicated larger aperture is shifted towards larger diode numbers with respect to the spectrum from the smaller aperture. Negative offsets indicate a shift towards smaller diode numbers. The average of the hot and cold offsets for

the blue tube are also listed in Table 3. The total error, σ_{tot}, is determined by

$$\sigma_{tot}^2 = \frac{1}{\sum_i \frac{1}{\sigma_{\overline{x}i}^2}}$$

where $\sigma_{\overline{x}i}$ are the errors in the mean of the hot and cold offsets. For all the aperture combinations listed in Tables 2, 3 and 4 (*i.e.* offsets between like aperture locations), no significant differential offsets are present.

The errors in the offsets of the prism data are about a factor of 10 larger than the grating data, because the prism spectrum has fewer sharp features. The brighter lines of the prism spectra overflow the 16 bit counters reducing the number of useful bins for cross-correlation to three or four. The offsets determined from the prism are in good agreement with those from G570H on the red side. The mean difference between the prism and G570H offsets is +0.006 diode with an error in the mean of ±0.006 diode. On the blue side, however, the mean difference is +0.029 diode with an error in the mean of ±0.006. For both tubes, the inconsistent offsets from the 2.0 × 2.0–Bar aperture were excluded from the computation of the means. The discrepancy on the blue side is probably caused by a difference in the uniformity of the illumination of the apertures between the internal and external calibration lamps. The G130H data was obtained with the internal Pt-Cr-Ne lamp and the blue prism data with the external Pt-Cr-Ne Lamp. The fact that the observed differences are large for the large apertures and a factor of 4 smaller for the small apertures suggests that the apertures were illuminated differently by the internal and external lamps. Therefore, only the blue side offsets for the internal lamps in Table 3 may be applicable to flight data.

The offsets listed in Tables 2, 3, and 4 clearly indicate that when the aperture positions in X are determined using calibration lamps, the centers of like aperture locations are not exactly concentric. Either the aperture wheel does not position precisely and/or there is a slight non–uniform illumination of the apertures by the lamps.

IV. Overall Wavelength Calibration Strategy

Wavelength scales are needed for all science spectra, but the method of obtaining wavelengths depends on whether or not a wavelength calibration spectrum is obtained without moving the filter–grating wheel (FGW). In the *first method*, no calibration spectrum is taken with the science spectrum and the wavelength scale is simply determined using mean

dispersion coefficients for the appropriate aperture and grating combination. The error in the wavelength scale from this approach is dominated by the FGW non–repeatability ($\approx \pm 0.2$ diode, Hartig 1985) and errors due to thermal effects (≈ 0.15 diode, Sirk and Bohlin 1986). The 0.004 diode aperture wheel non–repeatability may be neglected. The *second method* involves taking a calibration spectrum just before or after the science spectrum through the same aperture as the science spectrum and without moving the FGW or the aperture wheel. The calibration spectrum is then cross–correlated using the procedure outlined above in section II with a long exposure reference template spectrum obtained with the appropriate small aperture. Using the results of the cross–correlation, the positions of the spectral features on the calibration spectrum are reduced to the system of the reference spectrum, which has well determined dispersion coefficients. The shift between the template and calibration spectra may have non–constant shifts due to the thermal effects that are shown in Figure 6 of Sirk and Bohlin (1986), for example. In this case of shifts that are a function of diode position, the correction to the wavelengths should be determined by a low order polynomial fit to the offsets as a function of diode position. The advantages realized by cross–correlating calibration spectra with template spectra are that the FGW non-repeatability, the offsets between different apertures, the aperture wheel non-repeatability, and thermal effects are all eliminated by reducing the calibration spectrum to the system of a well calibrated reference spectrum. In addition, the exposure times for the calibration spectra may be reduced by a factor of 2.5, if cross–correlation is used rather than a direct calibration from identified spectral features. In principal, wavelength scales for all apertures with accuracies nearly equal to that of the smallest apertures will be possible.

The best estimates of absolute wavelengths for a science spectrum will be determined by applying the offset between the internal lamp and an external source to the wavelength scale found by the cross–correlation technique.

V. Conclusions

The aperture offsets for the blue tube using the internal lamp did not exceed 0.1 diode. The use of an external lamp on the blue side was consistent with the internal lamp to 0.03 diode. On the red side, offsets for an external lamp exceed 0.1 diode only for the 0.25×2.0 aperture. Thus, a typical offset for the relevant internal lamp on the red side is probably below 0.1 diode, in agreement with the blue side result.

In the case where no calibration lamp spectra is obtained with a science spectrum, the most accurate wavelengths are obtained from average template spectra and aperture offsets. However, the expected FGW repeatability is ±0.2 diode and will dominate the aperture offset corrections of up to 0.1 diode. Average template spectra will only reduce the wavelength uncertainty from ±0.4 to ±0.2 diode. Therefore, we recommend that routine data reduction should assume *zero* aperture offsets and that little effort be expended in getting average dispersion constants or appropriate aperture offsets. Considering typical thermal effects, the accuracy of wavelengths for science spectra unaccompanied by an internal lamp spectrum should be on the order of 0.5 diode.

In the case where a calibration lamp spectrum is obtained with a science spectrum, neither average template spectra nor aperture offsets are needed to achieve the most accurate wavelengths. Wavelength accuracy will probably be limited by pointing precision, but may approach the internal accuracy of 0.02 diode.

Currently, the pipeline data processing system cannot use a wavelength calibration spectrum to compute the wavelengths assigned to a science spectrum. Each observer would be required to do that computation. An improvement to the routine data processing at the STScI would be to implement the algorithms presented here to assign wavelengths to science spectra.

Table 2

Mean Aperture Offsets for the Red Tube (old F-3)
with Errors in the Means

Apertures	Mean Offset (diode)	$\sigma_{\bar{x}}$ (diode)	# Bins
	G570H Data Set		
0.1-PairL – 0.25-PairL	-0.037	.003	13
0.1-PairL – 0.5-PairL	-0.009	.002	11
0.1-PairL – 1.0-PairL	-0.031	.004	12
0.1-PairU – 0.25-PairU	-0.043	.001	11
0.1-PairU – 0.5-PairU	-0.014	.002	14
0.1-PairU – 1.0-PairU	-0.034	.003	11
0.3 – 0.5	0.032	.001	12
0.3 – 1.0	0.022	.003	14
0.3 – 0.25×2.0	-0.167	.003	14
0.3 – 0.7×2.0-Bar	-0.089	.003	12
0.3 – 2.0×2.0-Bar	-0.120	.020	18
	PRISM Data Set		
0.1-PairL – 0.25-PairL	-0.055	.010	4
0.1-PairL – 0.5-PairL	0.005	.009	4
0.1-PairL – 1.0-PairL	-0.059	.032	4
0.1-PairU – 0.25-PairU	-0.037	.012	3
0.1-PairU – 0.5-PairU	-0.005	.009	3
0.1-PairU – 1.0-PairU	0.000	.016	3
0.3 – 0.5	0.051	.027	4
0.3 – 1.0	0.017	.017	4
0.3 – 0.25×2.0	-0.130	.023	4
0.3 – 0.7×2.0-Bar	-0.095	.053	3
0.3 – 2.0×2.0-Bar	-0.003	.005	3

Table 3

Mean Aperture Offsets for the Blue Tube from the G130H
Cold and Hot data sets with Errors in the Means

Apertures	Cold			Hot			Average	
	Mean Offset†	$\sigma_{\overline{x}}$	# Bins	Mean Offset	$\sigma_{\overline{x}}$	# Bins	Average Offset	σ_{tot}
0.1-PairL – 0.25-PairL	−0.056	.004	16	−0.042	.007	17	−0.049	.003
0.1-PairL – 0.5-PairL	−0.088	.007	16	−0.064	.010	16	−0.076	.006
0.1-PairL – 1.0-PairL	0.011	.007	18	−0.002	.004	15	0.004	.003
0.1-PairU – 0.25-PairU	−0.062	.005	17	−0.068	.007	16	−0.065	.004
0.1-PairU – 0.5-PairU	−0.079	.010	16	−0.093	.005	12	−0.086	.005
0.1-PairU – 1.0-PairU	0.002	.007	16	0.004	.007	15	0.003	.005
0.3 – 0.5	0.037	.007	15	0.039	.004	14	0.038	.003
0.3 – 1.0	0.006	.004	15	−0.002	.003	14	0.002	.003
0.3 – 0.25×2.0	0.003	.005	17	−0.010	.007	13	−0.004	.004
0.3 – 0.7×2.0-Bar	0.036	.008	16	0.029	.004	14	0.032	.004
0.3 – 2.0×2.0-Bar	−0.019	.015	18	−0.066	.016	16	−0.042	.011

†All offsets and errors are in diodes.

Table 4

Mean Aperture Offsets for the Blue Tube

PRISM Data Set with Errors in the Means

Apertures	Mean Offset (diode)	$\sigma_{\overline{x}}$ (diode)	# Bins
0.1-PairL – 0.25-PairL	-0.041	.005	3
0.1-PairL – 0.5-PairL	-0.064	.014	3
0.1-PairL – 1.0-PairL	0.065	.023	3
0.1-PairU – 0.25-PairU	-0.049	.005	3
0.1-PairU – 0.5-PairU	-0.068	.013	3
0.1-PairU – 1.0-PairU	0.063	.019	3
0.3 – 0.5	0.056	.008	3
0.3 – 1.0	0.032	.009	3
0.3 – 0.25×2.0	0.013	.002	3
0.3 – 0.7×2.0-Bar	0.083	.018	3
0.3 – 2.0×2.0-Bar	0.028	.008	3

References

Hartig, G. 1985, *Improvements in Filter–Grating Wheel Repeatability* CAL/FOS–017, May 23, 1985, STScI.

Sirk, M., and Bohlin, R. 1986, *FOS Wavelength Calibration* CAL/FOS–026, February 1986, STScI.

Wheatley, J., Ford, H., and Bohlin, R. 1984, *FOS Aperture Wheel Repeatability and Filter–Grating Wheel Repeatability* CAL/FOS–008, May 1984, STScI.

Figure Captions

Figure 1. Caption with figure.

Figure 2. Aperture offset *vs.* Diode Number for G130H, blue tube, comparing the 0.25-PairL to the 0.25-PairU apertures. The (+) symbols are good points, and the (×) symbols are rejected points according to the data restrictions described in the text. The dashed line is the least squares fit to the good points. The significant slope indicates a differential offset along the diode array.

Figure 3. Aperture offset *vs.* Diode Number for G570H, red tube, comparing the 0.25-PairL to the 0.25-PairU apertures. The symbols are as for Figure 2.

Figure 4. Aperture offset *vs.* Diode Number for G130H, blue tube, comparing the 0.1-PairL to the 0.25-PairL apertures, as for Figure 2. The insignificant slope indicates that the offset is constant along the length of the diode array.

Figure 5. Aperture offset *vs.* Diode Number for G570H, red tube, comparing the 0.1-PairL to the 0.5-PairL apertures, as for Figure 2. There is no significant slope to the least squares line fit.

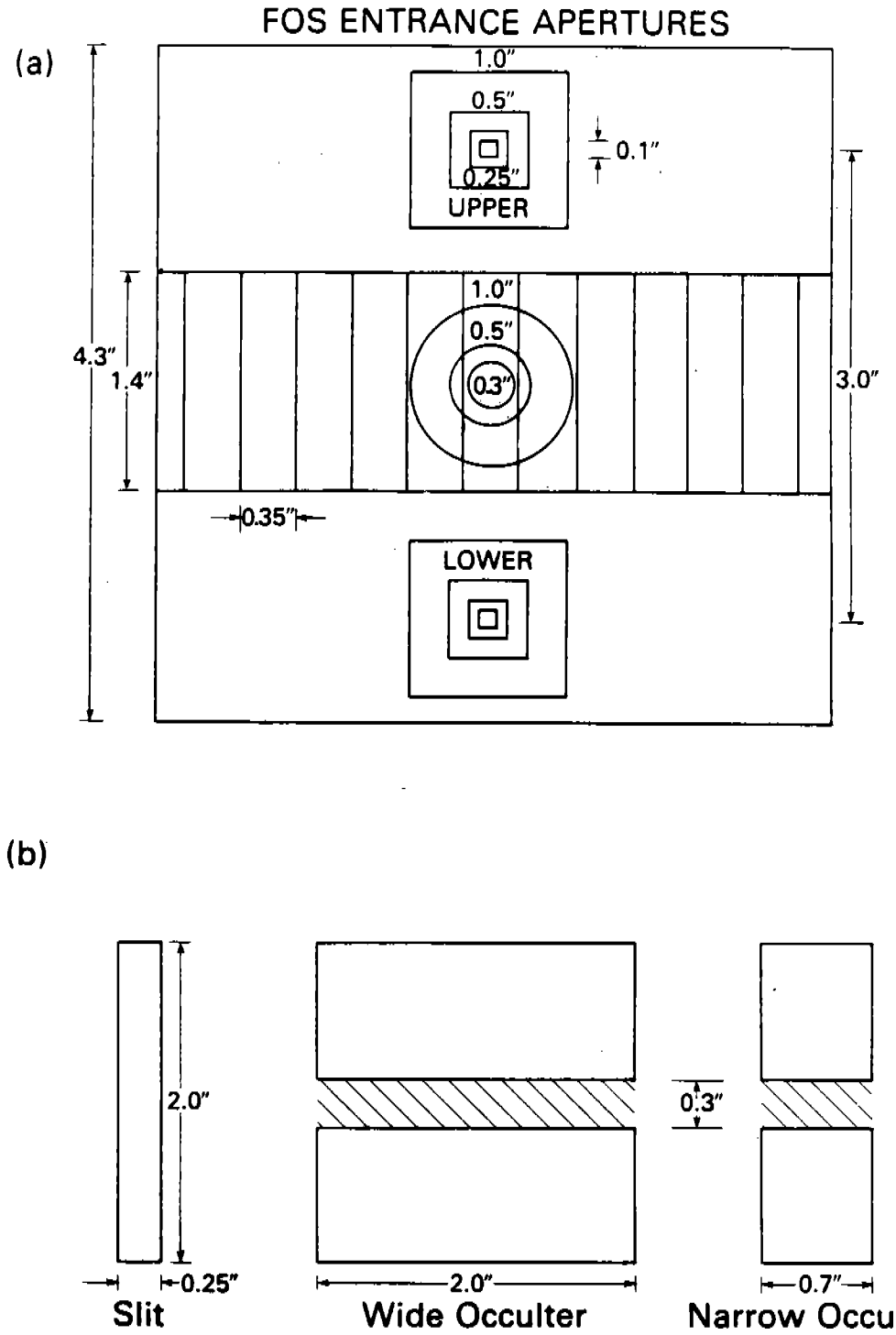

Figure 1. A Schematic of the FOS Apertures projected onto the sky. The upper panel shows the array of $0.35'' \times 1.4''$ diodes projected across the center of the $4.3'' \times 4.3''$ target acquisition aperture. The target acquisition aperture and the single circular apertures position to a common center. The pairs of square apertures position to common centers with respect to the target acquisition aperture as shown in the figure. Either the upper aperture (the "A" aperture, which is furtherest from the HST optical axis) or the lower aperture (the "B" aperture, which is closest to the HST optical axis) in a pair can be selected by an appropriate y-deflection in the Digicon detectors. The lower panel shows the three rectangular slits; two of the slits are bisected by an $0.3''$ opaque occulting bar. The centers of the three slits position to the center of the target acquisition aperture.

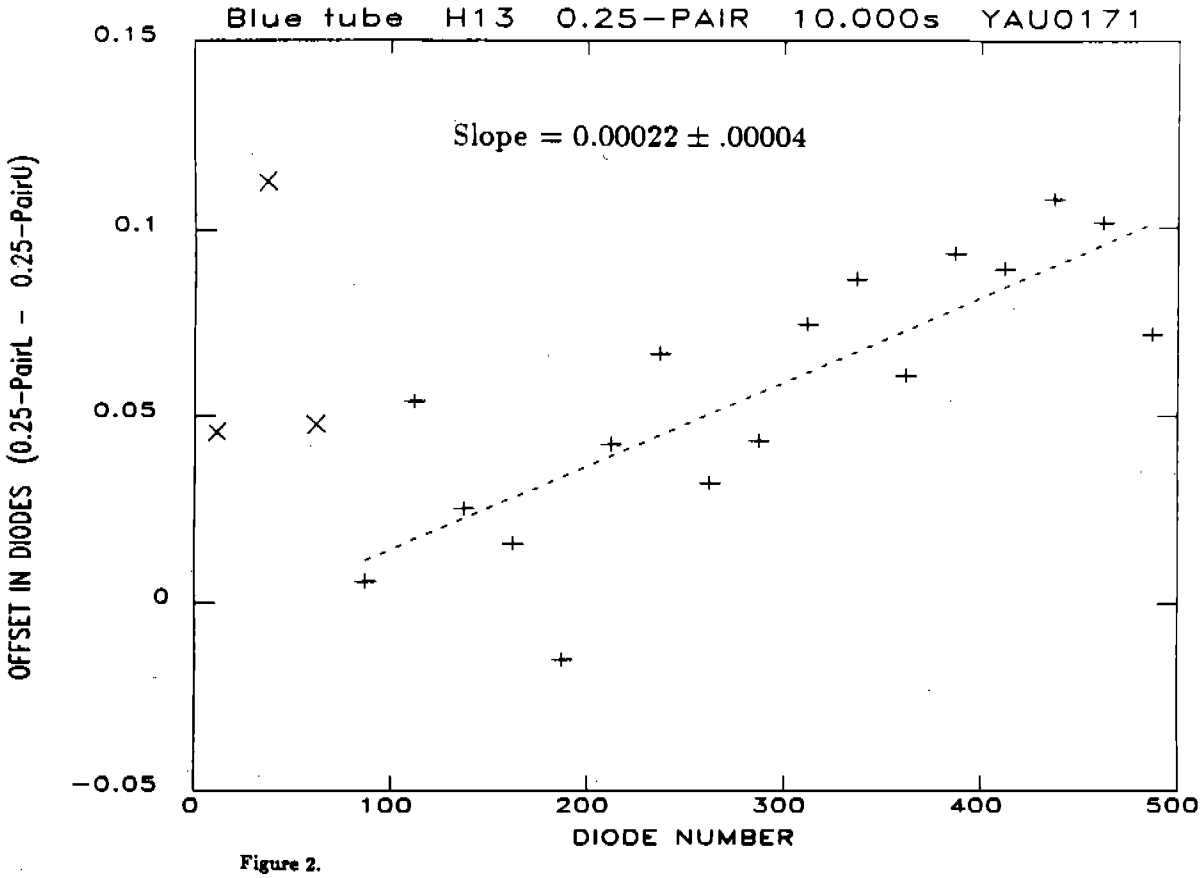

Figure 2.

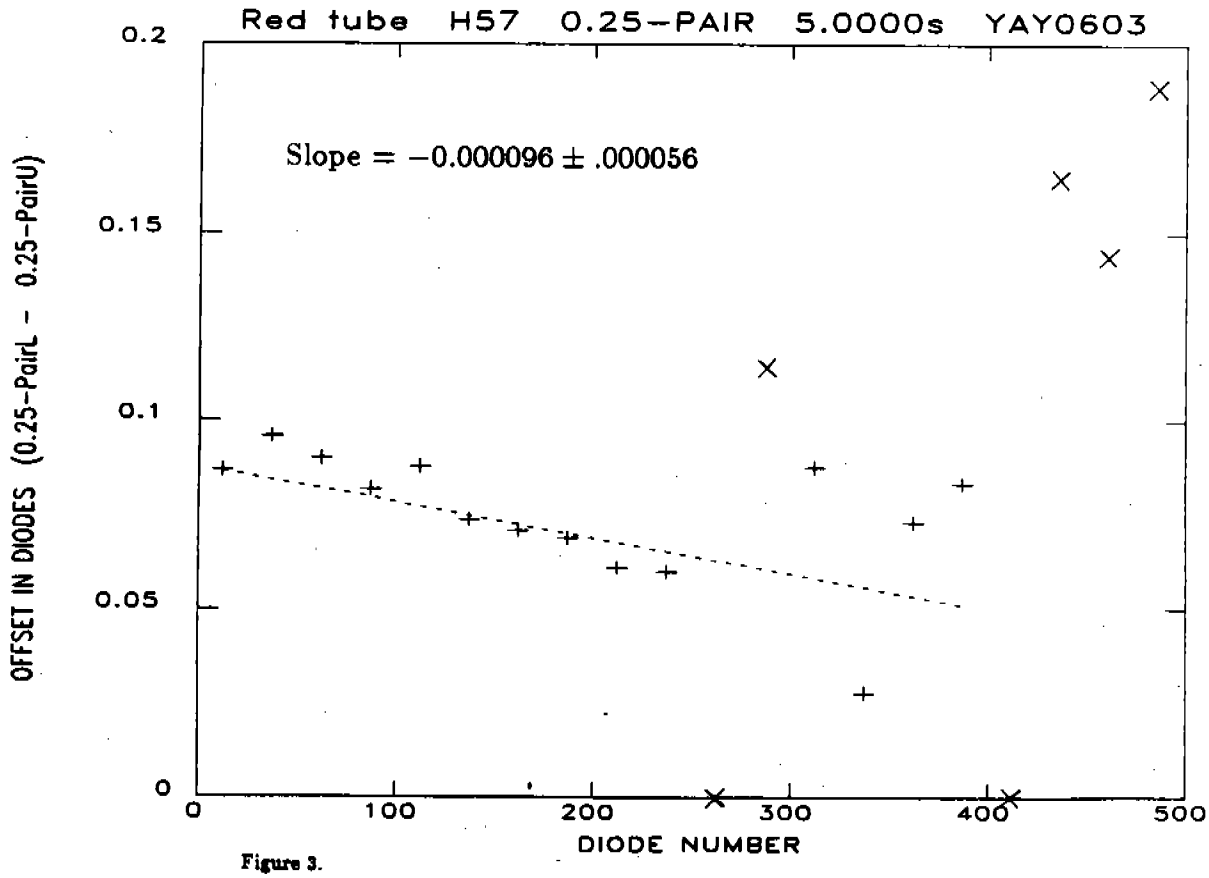

Figure 3.

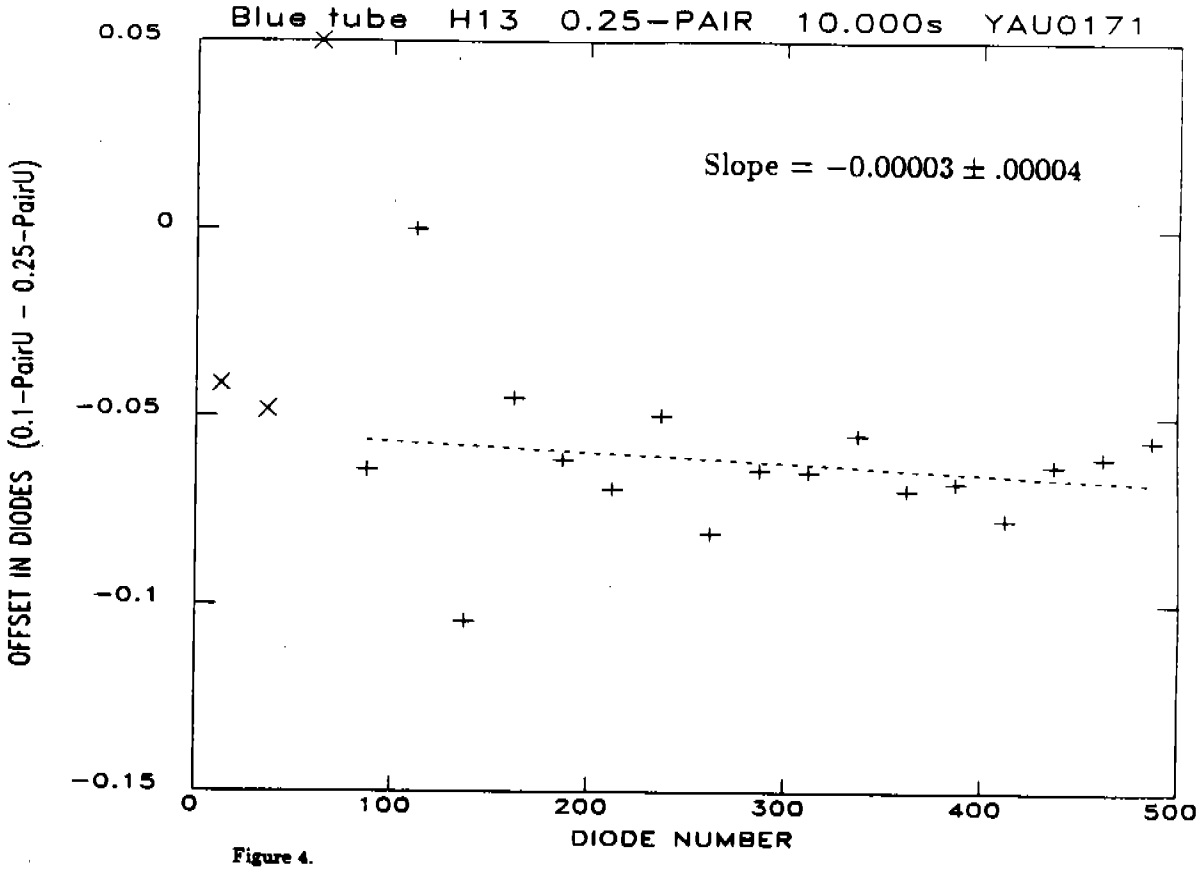

Figure 4.

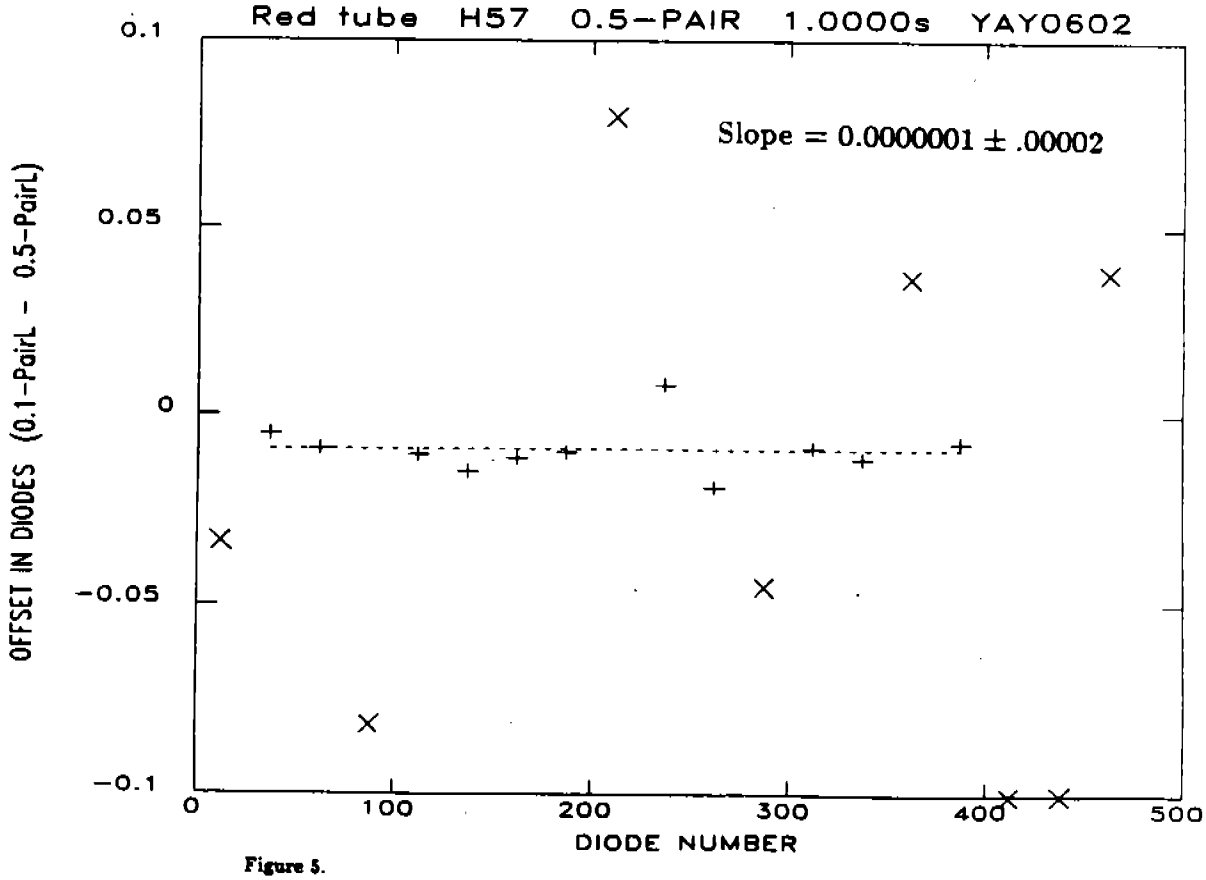

Figure 5.